THE ASTROPHYSICAL JOURNAL, 248:161–176, 1981 August 15

THE OOSTERHOFF PERIOD GROUPS AND THE AGE OF GLOBULAR CLUSTERS. II. PROPERTIES OF RR LYRAE STARS IN SIX CLUSTERS: THE *P-L-A* RELATION

ALLAN SANDAGE
Mount Wilson and Las Campanas Observatories of the Carnegie Institution of Washington
Received 1980 November 7; accepted 1981 February 3

ABSTRACT

Data for RR Lyrae stars in six clusters are used to test the conclusion of Paper I that, at *every temperature*, period shifts exist between variables in one cluster relative to those in another of a different Oosterhoff group. Variables in M3, M4, M15, NGC 6171, NGC 6891, and ω Cen have the same shifts in the period-temperature as in the period-amplitude relations; no shifts occur in the temperature-amplitude relation.

The period residuals, $\Delta \log P$, determined for individual stars in M3 and in ω Cen, correlate with their observed apparent magnitudes; hence, the observed spread in L_{RR} is real. Brighter variables than others in the same cluster have longer periods at fixed T_e or A. The data are consistent with $\Delta M_{bol} \approx 3\Delta \log P$ expected from $P\langle\rho\rangle^{1/2} = constant$ at fixed mass.

Combining the period deviations at fixed amplitude with the observed magnitude variations leads to a period-luminosity-amplitude relation for equal metallicity *ab* RR Lyrae variables of the form $M_{bol} = M_{bol}(M3_{15.52}) - 3(\log P + 0.129A_B + 0.088)$, where $M_{bol}(M3_{15.52})$ is the absolute magnitude of RR Lyrae stars in M3 that have $m_{bol} = 15.52$. The coefficient of the period-amplitude term will be −4.2 rather than −3 if mass is a function of metallicity as predicted by the models.

Subject headings: clusters: globular — stars: abundances — stars: evolution — stars: pulsation stars: RR Lyrae

I. INTRODUCTION

Using the $P\langle\rho\rangle^{1/2} = Q(M, L, Y, Z, T_e)$ relation for RR Lyrae variables applied to M3 and M15, it was shown in Paper I (Sandage, Katem, and Sandage 1981, hereafter SKS) that the relative shift toward longer periods in M15 at a given temperature requires either that (1) RR Lyrae stars in M15 are brighter than those in M3 by $\Delta M_{bol} \approx 3\Delta \log P$, (2) the masses of the M15 variables are smaller than those in M3 by $\Delta \log M \approx 1.5\Delta \log P$, or (3) some combination of the two. It was further shown that the predicted variation of mass with metallicity along the zero age horizontal branch (ZAHB) is of opposite sign to that required by item (2), and hence that the M15 ZAHB must be even brighter relative to M3 than $3\Delta \log P$ to explain the observed period shift.

The data in Paper I were also used to demonstrate (1) the same period shift obtained from the P-T_e relation exists between M15 and M3 variables in the period-amplitude relation, and (2) the color-amplitude relations coincide. This latter requires that amplitude is a function primarily of position within the instability strip.

These facts require the existence of a period-luminosity-amplitude (*P-L-A*) relation for RR Lyrae variables. The form of the function can be found (Sandage 1981*a*) by using individual variables that are brighter than others in the same cluster.

These results are generalized in the present paper to four other clusters where similar color data exist. The observations for RR Lyrae stars in M3, NGC 6121, NGC 6171, NGC 6981, and ω Cen are discussed in § II; correlations between period, temperature, amplitude, and rise times are given in § III, where, as in Paper I, a comparison is made with a model of the Oosterhoff period shifts. The intrinsic dispersion in luminosity and mass among variables in a given cluster is discussed in § IV. The data for M3 and ω Cen are used in § V to show again the existence of the *P-L-A* relation. Finally, this formulation of the *P-L-A* relation for RR Lyrae stars is shown in § VI to be similar in principle to that required for the long period Cepheids.

II. THE DATA

The needed observational data, together with additional parameters derived from them, are listed in Tables 1–6 for five clusters, discussed individually in the next subsections.

a) M3

The data in Table 1 are based on photometry by Roberts and Sandage (1955), Baker and Baker (1956), and Sandage (1959). Contamination corrections, derived from the data themselves, have been applied. These

TABLE 1

PARAMETERS FOR RR LYRAE STARS IN M3

No.	r''	P	$\log P$	$\langle V\rangle^c$	$[\langle B\rangle-\langle V\rangle]^c$	$[\langle U\rangle-\langle B\rangle]^c$	$\langle B-V\rangle^c_{mag}$	A_B	Δp_{rise}	$\log T_e^B(1)$	$\log T_e^B(2)$	m_{bol}	$\Delta \log P$ (O—C)
(1)	(2)	(3)	(4)	(5)	(6)	(7)	(8)	(9)	(10)	(11)	(12)	(13)	(14)
1	129	0.5206	-0.283	15.67	0.28	0.06	0.34	1.33	0.10	3.822	3.843	15.64	-0.023
6	138	0.5143	-0.289	15.77	0.31	0.01	0.40	1.21	(0.08)	3.799	3.832	15.76	-0.059
9	358	0.5415	-0.266	15.69	0.28	0.03	0.37	1.42	0.08	3.810	3.843	15.67	+0.012
12	146	0.3178	-0.498	15.67	0.20	0.12	0.22	0.62	0.40	3.863	3.869	15.60	. . .
16	316	0.5115	-0.291	15.72	0.28	0.04	0.34	1.46	0.10	3.822	3.843	15.69	-0.009
18	311	0.5163	-0.287	15.71	0.31	0.08	0.37	1.30	0.10	3.810	3.832	15.69	-0.037
19	428	0.6319	-0.199	15.69	0.42	-0.04	0.45	0.47	0.15	3.779	3.791	15.69	-0.058
21	347	0.5157	-0.288	15.70	0.30	-0.01	0.36	1.28	0.11	3.814	3.836	15.67	-0.043
24	148	0.6633	-0.178	15.58	0.39	0.04	0.42	0.85	0.16	3.791	3.803	15.57	+0.014
25	128	0.4800	-0.319	15.74	0.26	. . .	0.31	1.42	0.12	3.824	3.849	15.69	+0.009
26	182	0.5977	-0.223	15.63	0.29	(0.04)	0.34	1.35	0.13	3.822	3.839	15.60	+0.037
27	151	0.5790	-0.237	15.70	0.37	-0.01	0.40	0.94	(0.15)	3.799	3.810	15.69	-0.037
34	218	0.5591	-0.253	15.68	0.35	-0.01	0.37	0.59	0.20	3.810	3.818	15.66	-0.091
36	176	0.5455	-0.263	15.67	0.27	0.11	0.34	1.33	0.09	3.822	3.846	15.64	-0.003
37	288	0.3266	-0.486	15.66	0.24	0.03	0.26	0.61	0.32	3.849	3.856	15.60	. . .
40	294	0.5515	-0.258	15.70	0.31	(0.05)	0.36	1.27	0.12	3.814	3.832	15.67	-0.016
46	138	0.6133	-0.212	15.72	0.40	. . .	0.42	0.68	0.20	3.791	3.799	15.71	-0.040
48	163	0.6278	-0.202	15.57	0.39	-0.03	0.42	0.66	0.17	3.791	3.803	15.56	+0.032
51	228	0.5839	-0.234	15.69	0.32	0.07	0.37	1.18	0.12	3.810	3.829	15.67	-0.009
55	383	0.5298	-0.276	15.68	0.29	. . .	0.36	1.42	0.09	3.814	3.839	15.66	+0.002
56	385	0.3295	-0.482	15.64	0.23	0.05	0.25	0.65	0.28	3.853	3.860	15.58	. . .
60	434	0.7077	-0.150	15.55	0.38	. . .	0.40	0.73	0.20	3.799	3.806	15.54	+0.030
64	350	0.6054	-0.218	15.67	0.35	0.03	0.38	0.95	0.17	3.806	3.818	15.65	-0.018
65	351	0.6683	-0.175	15.52	0.33	0.02	0.36	1.16	0.17	3.814	3.825	15.50	+0.047
71	161	0.5490	-0.260	15.73	0.30	0.06	0.33	1.11	0.15	3.825	3.836	15.70	-0.041
72	446	0.4560	-0.341	15.69	0.25	0.06	0.31	1.63	0.11	3.832	3.853	15.65	. . .
74	175	0.4921	-0.308	15.71	0.25	. . .	0.32	1.47	0.09	3.829	3.853	15.67	-0.026
75	167	0.3140	-0.503	15.70	0.23	0.05	0.25	0.59	0.35	3.853	3.860	15.64	. . .
83	456	0.5012	-0.300	15.68	0.30	. . .	0.36	1.42	0.11	3.814	3.836	15.66	-0.024
84	177	0.5957	-0.225	15.67	0.39	-0.01	0.33	0.94	0.14	3.825	3.803	15.64	-0.025
85	380	0.3558	-0.499	15.52	0.18	0.09	0.20	0.64	0.40	3.869	3.876	15.45	. . .
90	212	0.5170	-0.286	15.68	0.32	. . .	0.38	1.38	0.11	3.806	3.829	15.66	-0.022
93	509	0.6023	-0.220	15.65	0.38	. . .	0.41	0.97	0.15	3.795	3.806	15.64	-0.020
94	538	0.5236	-0.281	15.70	0.25	. . .	0.30	1.39	0.12	3.836	3.853	15.66	-0.015
96	286	0.4994	-0.302	15.56	0.26	. . .	0.33	1.49	0.09	3.825	3.849	15.53	-0.010
105	193	0.2877	-0.541	15.60	0.18	0.10	0.20	0.39	0.35	3.869	3.876	15.53	. . .
107	344	0.3090	-0.510	15.66	0.21	0.08	0.23	0.67	0.30	3.860	3.866	15.59	. . .
108	380	0.5196	-0.284	15.71	0.28	0.03	0.32	1.36	0.14	3.829	3.843	15.67	-0.022
119	275	0.5177	-0.286	15.64	0.25	0.07	0.31	1.48	0.11	3.832	3.853	15.60	+0.004
120	376	0.6401	-0.194	15.66	0.40	-0.03	0.42	0.56	0.19	3.791	3.799	15.66	-0.036
124	212	0.7524	-0.124	15.57	0.40	. . .	0.42	0.42	0.28	3.791	3.799	15.57	+0.006
125	229	0.3498	-0.456	15.68	0.25	0.01	0.27	0.53	0.36	3.846	3.853	15.63	. . .
126	147	0.3484	-0.458	15.73	0.26	0.06	0.28	0.52	0.42	3.843	3.849	15.68	. . .
140	110	0.3331	-0.477	15.65	0.23	. . .	0.25	0.53	0.30	3.853	3.860	15.59	. . .
C	318	0.2871	-0.542	15.60	0.19	0.09	0.21	0.16	0.45	3.866	3.872	15.53	. . .
I-42	357	0.9163	-0.038	15.58	0.42	-0.02	0.44	0.14	(0.40)	3.783	3.791	15.58	. . .
I-100	195	0.998	-0.001	(15.60)	0.41	. . .	0.42	0.15	(0.40)	3.791	3.795	(15.60)	. . .

TABLE 2

RISE TIMES FOR ADDITIONAL M3 VARIABLES

No. (1)	P (2)	log P (3)	$\Delta\varphi_{rise}$ (4)
10 ...	0.5695	−0.245	0.11
11 ...	0.5078	−0.294	≤0.08
13 ...	0.4830	−0.316	≤0.13
14 ...	0.6358	−0.197	(0.15)
20 ...	0.4912	−0.309	(0.18)
28 ...	0.4706	−0.327	0.12
39 ...	0.5870	−0.231	(0.17)
45 ...	0.5368	−0.270	0.12
50 ...	0.5130	−0.290	(0.17)
57 ...	0.5123	−0.291	≤0.10
59 ...	0.5888	−0.230	(0.20)
61 ...	0.5209	−0.283	0.14
62 ...	0.6524	−0.185	0.16
63 ...	0.5704	−0.244	0.10
66 ...	0.6201	−0.207	(0.22)
67 ...	0.5683	−0.245	0.17
79 ...	0.4832	−0.316	(0.20)
81 ...	0.5291	−0.276	0.14
86 ...	0.2926	−0.534	0.32
87 ...	0.3574	−0.447	0.35
97 ...	0.3349	−0.475	0.37
117 ...	0.6005	−0.221	0.10
118 ...	0.4993	−0.302	0.10
128 ...	0.2922	−0.534	0.24

corrections, taken from the ridge lines of Figure 1, are based on the change of color and magnitude with radial distance from the cluster center for the variables listed in Table V of Roberts and Sandage.

Table 1 contains the following data. The name of the variable, its radial distance, and its period in columns (1)–(3) are from the Second and Third Catalogs of Variable Stars in Clusters (Hogg 1955, 1973). The contamination-corrected V magnitudes and colors, based on the sources previously mentioned, are in columns (5)–(7). The mean colors in column (8) are determined from integrations of the color curves expressed in magnitudes, using data from column (6) and Figure 1 of Preston (1961). The reddening is assumed to be $E(B-V)=0.00$ (Sandage 1969). The blue amplitude from Roberts and Sandage is in column (9). The rise time, defined as in Paper I as the fraction of the period between minimum and maximum, is in column (10). The T_e (1) temperatures in column (11) are based on an unpublished color-temperature calibration of Bell quoted by Butler, Dickens, and Epps (1978) using the $\langle B-V\rangle_0^c$ mag colors in column (8). The T_e (2) temperatures in column (12) are from the same calibration, but use the $[\langle B\rangle-\langle V\rangle]_0^c$ system of colors. The apparent bolometric magnitudes in column (13) are obtained by applying Bell's bolometric corrections tabulated by Butler *et al.* to the

TABLE 3

PARAMETERS FOR RR LYRAE STARS IN NGC 6121[a]

No. (1)	r'' (2)	P (3)	log P (4)	δE (5)	$\langle V\rangle-3\delta E$ (6)	$\frac{[\langle B\rangle-\langle V\rangle]^o}{\delta E}$ (7)	$\frac{\langle B-V\rangle_{mag}}{\delta E}$ (8)	A_B (9)	$\Delta\varphi_{rise}$ (10)	T_e^b(2) (11)
2	315	0.5356	-0.271	+0.07	13.23	0.28	0.31	1.37	0.16	3.847
5	207	0.6223	-0.206	-0.02	13.39	0.40	0.42	0.43	0.22	3.806
6	338	0.3205	-0.494	. . .	(13.49)	(0.24)	(0.26)	0.61	(0.34)	3.860
7	257	0.4987	-0.302	+0.01	13.42	0.31	0.36	1.22	≤0.12	3.837
11	304	0.4930	-0.307	-0.02	13.52	0.35	0.39	1.02	<0.18	3.823
12	214	0.4461	-0.351	+0.03	13.47	0.27	0.34	1.55	<<0.23	3.851
14	248	0.4635	-0.334	+0.09	13.36	0.25	0.32	1.58	0.09	3.857
15	437	0.4437	-0.353	+0.05	13.33	0.26	0.33	1.54	0.09	3.854
19	358	0.4678	-0.330	+0.04	13.20	0.26	0.32	1.48	≤0.11	3.854
27	281	0.6120	-0.213	+0.03	13.13	0.31	0.34	1.22	0.15	3.837
28	272	0.5223	-0.282	-0.04	13.29	0.31	0.36	1.24	∿0.12	3.837
29	681	0.5224	-0.282	-0.01	13.35	0.31	0.36	1.24	0.12	3.837
30	347	0.2697	-0.569	. . .	(13.34)	(0.18)	(0.20)	0.75	(0.40)	3.880
31	356	0.5053	-0.296	-0.02	13.25	0.28	0.31	1.38	0.15	3.847
32	747	0.5791	-0.237	-0.03	13.27	0.35	0.40	1.02	0.13	3.823
33	1022	0.6148	-0.211	-0.03	13.11	0.31	0.35	1.21	0.14	3.837
35	382	0.6270	-0.203	+0.04	13.27	0.38	0.41	0.78	0.16	3.813
42	673	0.3037	-0.518	. . .	(13.25)	(0.19)	(0.21)	0.53	0.37	3.876
43	1306	0.3206	-0.494	. . .	(13.08)	(0.18)	(0.20)	0.59	0.32	3.880

[a]Photometric data based on photoelectric observations by Sturch (1977) and by Cacciari (1979).

[b]Temperatures based on E(B-V) = 0.36 + δE and the scale of Butler et al. (1978) appropriate for [Fe/H] = -1.0, using [⟨B⟩-⟨V⟩]° + δE colors of column (7).

TABLE 4

PARAMETERS FOR RR LYRAE STARS IN NGC 6171[a]

No.	r''	P	log P	$\langle V\rangle^c$	$[\langle B\rangle-\langle V\rangle]^o$	$[\langle U\rangle-\langle B\rangle]^o$	$\langle B-V\rangle^o_{mag}$	A_B	$\Delta\varphi_{rise}$	log T_e^b(1)	log T_e^b(2)
(1)	(2)	(3)	(4)	(5)	(6)	(7)	(8)	(9)	(10)	(11)	(12)
1	534	0.3233	-0.490	15.62	0.29	0.22	0.31	0.57	0.50	3.846	3.852
2	416	0.5710	-0.243	15.64	0.42	0.12	0.45	1.03	0.17	3.801	3.812
3	290	0.5663	-0.247	15.43	0.41	0.18	0.43	0.69	0.24	3.808	3.814
4	186	0.2821	-0.550	15.55	0.20	0.19	0.22	0.66	0.33	3.872	3.878
5	282	0.7024	-0.153	15.52	0.48	0.21	0.50	0.57	0.32	3.784	3.791
6	68	0.2602	-0.585	15.58	0.23	0.25	0.25	0.65	0.25	3.863	3.869
7	74	0.4996	-0.301	15.65	0.44	0.20	0.47	1.04	0.16:	3.794	3.805
8	44	0.5599	-0.252	15.57	0.41	0.22	0.44	1.35	0.15	3.805	3.814
9	33	0.3206	-0.494	15.63	0.35	0.20	0.37	0.62	0.40	3.827	3.834
10	58	0.4155	-0.381	15.79	0.33	0.18	0.38	1.40	0.12	3.824	3.840
11	34	0.5928	-0.227	15.71	0.51	0.19	0.54	0.81	0.18	3.770	3.780
12	85	0.4729	-0.325	15.69	0.36	0.16	0.39	1.31	0.15:	3.821	3.831
13	77	0.4668	-0.331	15.81	0.37	0.22	0.42	1.63	0.12	3.812	3.827
14	84	0.4816	-0.317	15.66	0.34	0.26	0.38	1.73	0.13	3.824	3.837
15	122	0.2886	-0.540	15.62	0.24	0.23	0.26	0.59	0.32	3.861	3.866
16	132	0.5228	-0.282	15.68	0.45	0.27	0.48	1.05	0.15	3.791	3.801
17	122	0.5611	-0.251	15.56	0.36	0.18	0.39	1.34	0.17	3.821	3.831
18	229	9.5643	-0.248	15.74	0.43	0.22	0.45	1.12	0.20	3.801	3.808
19	284	0.2787	-0.555	15.75	0.27	0.27	0.29	0.66	0.25	3.852	3.858
20	60	0.5781	-0.238	15.60	0.47	0.20	0.50	0.92	0.16	3.784	3.794

[a]Photometric data are based on observations by Dickens (1971) with the Mount Wilson 2.5 meter Hooker reflector.

[b]Temperatures based on E(B-V) = 0.28 and the scale of Butler et al. (1978) appropriate for [Fe/H] = -0.5. The T_e(1) scale of column (11) is based on $\langle B-V\rangle^o_{mag}$ colors in column (8). The T_e(2) scale of column (12) is based on $[\langle B\rangle-\langle V\rangle]^o$ colors in column (6).

TABLE 5

PARAMETERS FOR RR LYRAE STARS IN NGC 6981[a]

No.	r''	P	log P	$\langle V\rangle^o$	$[\langle B\rangle-\langle V\rangle]^{o,c}$	$\langle B-V\rangle^{o,c}_{mag}$	Δ_B	$\Delta\varphi_{rise}$	log T_e^b(1)	log T_e^b(2)
(1)	(2)	(3)	(4)	(5)	(6)	(7)	(8)	(9)	(10)	(11)
2	207	0.4652	-0.332	16.99	0.22	0.30	1.66	0.08	3.836	3.863
3	79	0.4976	-0.303	16.93	0.25	0.31	1.58	0.11	3.832	3.853
4	105	0.5524	-0.258	16.95	0.35	0.40	1.18	0.13	3.799	3.818
7	50	0.5246	-0.280	16.99	0.33	0.39	1.17	0.10	3.809	3.825
8	82	0.5683	-0.245	17.05	0.36	0.42	1.01	0.11	3.791	3.814
9	45	0.6029	-0.220	17.05	0.41	0.44	0.80	0.15	3.783	3.795
10	88	0.5581	-0.253	17.00	0.36	0.40	1.08	0.14	3.799	3.814
11	70	0.5199	-0.284	17.08	0.39	0.46	0.91	(0.09)	3.775	3.803
15	64	0.5504	-0.259	16.99	0.37	0.42	0.93	(0.12)	3.791	3.810
17	46	0.5735	-0.241	17.05	0.36	0.42	1.05	0.11	3.791	3.814
21	78	0.5311	-0.275	17.06	0.37	0.40	1.29	<0.15	3.799	3.810
23	144	0.5850	-0.233	17.00	0.43	0.49	0.78	0.10	3.763	3.787
25	139	0.3533	-0.452	16.92	0.24	0.26	0.56	0.32	3.849	3.856
27	308	(0.6737)	(-0.171)	16.74	0.28	0.30	1.49	. . .	3.836	3.843
28	97	0.5672	-0.246	16.97	0.37	0.40	0.81	∿0.16	3.799	3.810
29	65	0.6054	-0.218	16.94	0.39	0.42	0.80	0.16	3.791	3.803
32	137	0.5283	-0.277	17.01	0.35	0.40	0.94	. . .	3.799	3.818
35	222	0.5437	-0.265	17.01	0.35	0.39	0.97	<0.14	3.809	3.818

[a]Photometric data are based on observations by Dickens and Flinn (1972) with the Mount Wilson 2.5 meter Hooker reflector. The crowding corrections are severe.

[b]Temperatures based on $E(B-V)$ = 0.04 and the scale of Butler et al. (1970) appropriate for [Fe/H] = -1.5. The T_e(1) scale uses $\langle B-V\rangle^{o,c}_{mag}$ colors in column (7). The T_e (2) scale uses $[\langle B\rangle-\langle V\rangle]^{o,c}$ colors in column (6).

TABLE 6

PARAMETERS FOR RR LYRAE STARS IN ω CENTAURI

No.	P	Log P	A_B	$\Delta\omega_{rise}$	E=0.11 $[\langle B\rangle-\langle V\rangle]^o$	E=0.11 $\langle B-V\rangle^o_{mag}$	Log T_e^{BDE}	[Fe/H]	m_{bol}	Δlog P(O−C)
(1)	(2)	(3)	(4)	(5)	(6)	(7)	(8)	(9)	(10)	(11)
					-0.5 > [Fe/H] > -1.1; ⟨[Fe/H]⟩ = -0.80 ± 0.20σ					
3	0.841	-0.075	0.92	0.18	0.37	0.40	3.814	-1.06	14.33	+0.067
9	0.523	-0.281	0.97	0.17	0.28	0.31	3.851	-0.75	14.68	-0.131
44	0.567	-0.246	1.12	0.11	0.24	0.30	3.862	-0.87	14.57	-0.064
55	0.581	-0.235	1.01	0.13	0.32	0.37	3.836	-0.89	14.72	-0.075
67	0.564	-0.248	1.10	0.12	0.31	0.36	3.845	-0.58	14.59	-0.073
84c	0.579	-0.237	0.81	0.17	0.35	0.38	3.833	-0.51	14.22	. . .
99	0.766	-0.116	1.13	0.13	. . .	. . .	. . .	-1.04	. . .	. . .
125	0.592	-0.227	1.42	0.10	0.21	0.27	3.872	-0.69	14.51	+0.038
					-1.1 > [Fe/H] > -1.6; ⟨[Fe/H]⟩ = -1.34 ± 0.16σ					
4	0.627	-0.203	1.29	0.11	0.25	0.31	3.854	-1.29	14.46	+0.020
7	0.713	-0.147	1.13	0.14	0.32	0.36	3.827	-1.59	14.43	+0.035
13	0.669	-0.174	1.14	0.13:	0.29	0.34	3.839	-1.53	14.39	+0.010
27	0.615	-0.211	0.69	0.17	. . .	. . .	. . .	-1.16	. . .	. . .
32	0.620	-0.207	1.33	0.11	0.30	0.36	3.838	-1.17	14.37	+0.028
34	0.733	-0.134	0.95	0.15	0.33	0.36	3.827	-1.22	14.45	+0.016
45	0.589	-0.230	1.25	0.10	0.27	0.33	3.848	-1.14	14.44	-0.018
64	0.344	-0.463	0.57	0.28	0.23	0.25	3.860	-1.43	14.49	. . .
77	0.426	-0.371	0.48	0.5	0.28	0.30	3.842	-1.49	14.44	. . .
79	0.608	-0.216	1.30	0.10	0.25	0.31	3.853	-1.40	14.56	+0.010
83	0.356	-0.448	0.57	0.4	0.22	0.24	3.862	-1.58	14.50	. . .
85	0.742	-0.129	0.86	0.15	0.31	0.34	3.834	-1.16	14.44	+0.003
95	0.405	-0.393	0.49	0.5	0.30	0.32	3.836	-1.36	14.43	. . .
96	0.624	-0.204	0.89	0.12	. . .	. . .	. . .	-1.28	. . .	. . .
124	0.331	-0.479	0.60	0.25	0.18	0.20	3.876	-1.45	14.48	. . .
					-1.6 > [Fe/H] > -2.3; ⟨[Fe/H]⟩ = -1.88 ± 0.19σ					
5	0.515	-0.288	1.28	0.09	0.28	0.35	3.835	-2.13	14.78	-0.068
8	0.521	-0.283	1.39	0.11	0.20	0.26	3.869	-1.75	14.55	-0.029
10	0.374	-0.426	0.52	0.44	0.21	0.23	3.865	-1.65	14.45	. . .
14	0.377	-0.424	0.61	0.50	0.21	0.23	3.860	-2.09	14.49	. . .
18	0.621	-0.206	1.29	0.11	0.31	0.37	3.831	-1.76	14.44	+0.017
22	0.396	-0.402	0.54	0.42	0.26	0.28	3.841	-2.23	14.47	. . .
33	0.602	-0.220	1.36	0.11	0.30	0.36	3.827	-2.18	14.49	+0.025
36	0.379	-0.420	0.55	0.45	0.24	0.26	3.855	-1.85	14.42	. . .
38	0.779	-0.108	0.75	0.18	0.36	0.38	3.811	-1.69	14.50	+0.008
39	0.393	-0.405	0.56	0.5	0.19	0.21	3.867	-2.14	14.49	. . .
49	0.604	-0.219	1.12	0.12	0.36	0.41	3.806	-1.93	14.56	-0.038
56	0.568	-0.246	1.01	0.09	0.33	0.40	3.823	-1.64	14.72	-0.086
57	0.794	-0.100	0.75	0.16	0.35	0.38	3.816	-1.80	14.45	+0.015
63	0.825	-0.083	0.57	0.21	0.35	0.37	3.810	-1.98	14.48	+0.010
68c	0.534	-0.272	0.52	0.50	0.26	0.28	3.848	-1.79	14.19	. . .
69	0.653	-0.185	1.15	0.12	0.28	0.33	3.843	-1.68	14.51	+0.005
72	0.384	-0.415	0.52	0.43	0.23	0.25	3.852	-2.18	14.49	. . .
74	0.503	-0.298	1.49	0.11	0.24	0.30	3.854	-1.80	14.50	-0.006
76	0.337	-0.471	0.42	0.45	0.15	0.17	3.881	-1.94	14.52	. . .
104	0.867	-0.062	0.41	0.25	0.34	0.36	3.820	-1.61	14.43	+0.016
114	0.675	-0.171	0.75	0.12	. . .	. . .	. . .	-1.98	. . .	. . .
126	0.341	-0.466	0.52	0.15	0.19	0.22	3.872	-1.80	14.51	. . .
134	0.652	-0.185	1.27	0.10	0.27	0.33	3.844	-1.66	14.47	+0.033
160	0.397	-0.401	0.52	0.50	0.23	0.25	3.856	-1.86	14.49	. . .
163	0.313	-0.504	0.27	0.5	0.16	0.18	3.880	-1.92	14.49	. . .
					Unknown Metallicity					
16	0.330	-0.481	0.57	0.20	0.20	0.22	3.869	. . .	14.49	. . .
19	0.299	-0.524	0.54	0.35	0.20	0.22	3.869	. . .	14.79	. . .
24c	0.462	-0.335	0.47	0.50	0.33	0.35	3.825	. . .	14.38	. . .
46	0.686	-0.163	1.14	0.13	0.32	0.37	3.829	. . .	14.42	+0.022
47c	0.485	-0.314	0.46	0.5	0.32	0.34	3.828	. . .	14.18	. . .
50	0.386	-0.413	0.53	0.42	0.25	0.27	3.853	. . .	14.55	. . .
54	0.772	-0.112	0.83	0.19	0.35	0.37	3.818	. . .	14.37	+0.016
58	0.369	-0.432	0.25	0.5	0.17	0.19	3.879	. . .	14.47	. . .
70	0.390	-0.408	0.49	0.40	0.24	0.26	3.856	. . .	14.45	. . .
73	0.575	-0.240	1.31	0.12	0.28	0.33	3.843	. . .	14.47	-0.012
75c	0.422	-0.374	0.45	0.5	0.28	0.30	3.843	. . .	14.38	. . .
81	0.389	-0.410	0.52	0.5	0.26	0.28	3.849	. . .	14.48	. . .
82	0.335	-0.474	0.53	0.35	0.24	0.26	3.856	. . .	14.36	. . .
94	0.253	-0.595	0.31	0.38	0.17	0.19	3.879	. . .	14.68	. . .
101	0.340	-0.468	0.44	0.50	0.21	0.23	3.866	. . .	14.52	. . .
105	0.335	-0.475	0.55	0.5	0.24	0.26	3.855	. . .	14.60	. . .
115	0.630	-0.200	1.18	0.11	0.30	0.36	3.836	. . .	14.50	-0.005
123c	0.473	-0.324	0.49	0.50	0.26	0.28	3.849	. . .	14.43	. . .
127	0.305	-0.515	0.38	0.5	0.17	0.19	3.879	. . .	14.53	. . .
130	0.493	-0.307	1.10	0.12	0.23	0.28	3.860	. . .	14.58	. . .
149	0.682	-0.166	1.21	0.11	0.29	0.35	3.839	. . .	14.37	+0.036
151	0.407	-0.390	0.42	0.5	0.18	0.20	3.876	. . .	14.47	. . .

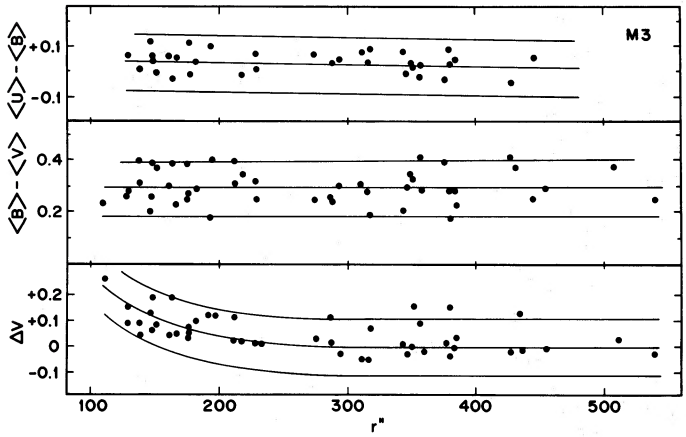

FIG. 1.—Contamination correction for M3, based on RR Lyrae data by Roberts and Sandage (1955). Distance from cluster center is the abscissa. The correction ΔV is normalized to be 0 beyond $r \approx 300''$. The observed colors are plotted in the upper two panels. No color corrections are needed.

magnitudes in column (5). Finally, the period shift $\Delta \log P$ of each variable relative to the mean fiducial period-amplitude relation for M3, (§ V, Fig. 11), is in column (14). The sense is that stars with longer periods than the fiducial line (at a fixed amplitude) have positive values of $\Delta \log P$.

Rise times for an additional 24 variables that were not discussed by Roberts and Sandage are given in Table 2, obtained from unpublished light curves using the original data.

b) NGC 6121

Data in Table 3 are derived from photoelectric photometry by Sturch (1977) and by Cacciari (1979) for 19 stars in M4. The variables are distant enough from the center that no correction for contamination is necessary. The table is self-explanatory except for columns (5)–(8). The cluster, at galactic latitude $b = +16°$, has variable reddening in its foreground. Study of the cluster *C-M* diagram and of the deviations of the variables in the color-amplitude and period-amplitude relations give reddenings of $E(B-V) = 0.36 + \delta E$, where δE is listed in column (5). the $\langle V \rangle$ measured by Sturch and Cacciari is corrected by $-3\delta E$ in column (6). Columns (7) and (8) give the adopted reddening-free colors. The temperature in column (11) is based on the colors in column (7) using the tabulation of Butler, Dickens, and Epps.

c) NGC 6171

Photoelectric data for the RR Lyrae variables in this metal-rich cluster are listed in Table 4, based on observations by Dickens (1971) made at Mount Wilson. Significant corrections for contamination have been applied to $\langle V \rangle$ for $r < 100''$, based on plots similar to those in Figure 1, but from the NGC 6171 data themselves. No corrections were necessary to the colors. Again, two temperature scales are listed: T_e (1) is based on $\langle B-V \rangle^{0,c}_{mag}$ colors of column (8); T_e (2) uses $[\langle B \rangle - \langle V \rangle]^0$ of column (6), both with an adopted reddening of $E(B-V) = 0.28$ (Sandage and Katem 1964; Dickens and Rolland 1972).

d) NGC 6981

Similar data for NGC 6981 from observations by Dickens and Flinn (1972) obtained at Mount Wilson, are given in Table 5. Very large contamination corrections are necessary for $r < 100''$, reaching $\Delta V = +0.3$ and $\Delta(B-V) = +0.2$ at $r = 30''$. Hence, these data are of lower weight than those for the other clusters. The two temperature scales are based on colors in columns (6) and (7) with an assumed reddening of $E(B-V) = 0.04$.

e) ω Centauri

Data for variables in ω Cen are listed in Table 6. The primary data are those summarized by Butler, Dickens, and Epps (1978), including their precepts for averaging the available values of [Fe/H].

The variables are separated in the table into three groups by metallicity, where known; otherwise they are listed at the end. The mean values of [Fe/H] are −0.80, −1.34, and −1.88 for the three groups. The amplitudes in column (4) are from Martin (1938). All other photometric values are from the new photometry by Butler *et al.* listed in their Table 1. Their temperatures and bolometric magnitudes are in columns (8) and (10). For later analysis of the *P-L-A* relation (§ V), the $\Delta \log P$ relative to an adopted fiducial *P-A* relation for ω Cen itself are given in column (11), using the same sign convention of *observed* minus *computed* as for M3.

The variables are far from the cluster center, and no contamination corrections are needed. The corrected colors are based on $E(B-V) = 0.11$, assumed to be constant over the cluster.

III. CORRELATIONS AMONG PERIOD, TEMPERATURE, AMPLITUDE, AND RISE TIMES

The requirement that the Oosterhoff period shifts are due to brighter absolute magnitudes for group II variables compared with group I is that all variables in a group II cluster must follow a different period-temperature relation than variables in group I. All periods must differ at a given temperature.[1] If, in addition, there is a unique amplitude and/or light curve shape associated with any given depth of penetration into the instability strip, the period-amplitude and period-rise time relations should also differ, but the amplitude-temperature relations should not.[2]

Although these requirements of the model (Sandage 1958*a*) were shown to hold between M3 and M15 (SKS), it is necessary that they hold for all clusters if this explanation of the Oosterhoff period groups is universal. The requirements are tested here using data for the four additional clusters.

Ritter's pulsation condition $P\langle\rho\rangle^{1/2}=Q$ to be tested in this way is

$$\log P+0.336m_{\rm bol}=-0.68\log M-3.48\log T_e+\text{const}, \quad (1)$$

which takes into account the variation of Q with composition, mass, and luminosity (van Albada and Baker 1971; Iben and Huchra 1972; Stellingwerf 1975). As in Paper I, we first neglect the mass term. The variations of mass within the instability strip of any cluster can then be studied subsequently by using the scatter in the $\log P+0.336\ m_{\rm bol}$, $\log T_e$ diagrams.

To avoid intrinsic scatter within a given cluster from increased luminosity due to evolution of its own variables, the diagrams are plotted using the reduced period $\log P+0.336\Delta m_{\rm bol}$ for each variable in a given cluster, where $\Delta m_{\rm bol}$ is taken relative to the mean $m_{\rm bol}$ in that cluster. Hence $\Sigma_i\Delta m^i_{\rm bol}\equiv 0$ within any cluster, and no bias is introduced in $\Delta\log P$ by applying this evolutionary correction.

Comparison of the reduced period-temperature relations for the six clusters is shown in Figure 2. The clusters are plotted in order of metallicity. The temperature scale is $T_e(2)$, based on $[\langle B\rangle-\langle V\rangle]$ colors.

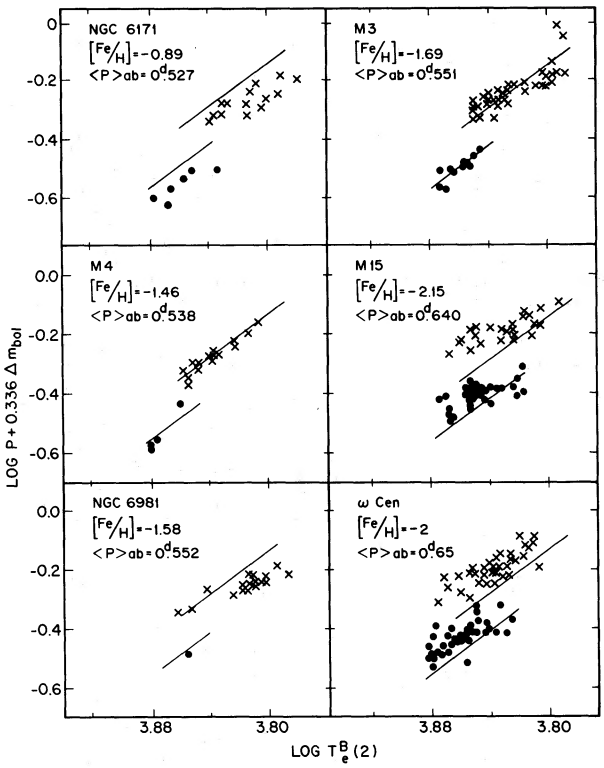

FIG. 2.—The reduced period-temperature relations for six clusters, arranged in order of [Fe/H]. The ordinate for each cluster has the same mean zero point as plots that use log P alone, hence the correction term for magnitude has been made to sum to zero exactly for each cluster. The temperature scale is based on $[\langle B\rangle-\langle V\rangle]^c_0$ colors, using a calibration by Bell. The lines have the theoretical slope of 3.48 from eq. (1) for constant mass. The M3 lines are repeated in all panels. Circles, type *c* variables; *crosses*, *ab* variables.

The lines, repeated from the M3 relation, are drawn in each panel to show the period shift at constant T_e, relative to M3. They have been put through the M3 data by eye with a forced slope of -3.48 from equation (1). The quoted metallicities are from Zinn (1980); the mean periods for *ab* variables are calculated from Hogg (1973). The *c* types are closed circles; the *ab* types are crosses.

The principal conclusion from Figure 2 is that, at any given T_e, *all* variables in a given cluster are shifted in period relative to those in M3 by about the amount suggested by their $\langle P\rangle_{ab}$ values. The periods of the NGC 6171 variables are shorter than those in M3 by $\Delta\log P\approx+0.060$; those in M4 and NGC 6981 are about the same as in M3; those in M15 and ω Cen are longer by $\Delta\log P\approx-0.055$. (The data for NGC 6981 suggest otherwise at first glance, but note that the M3 line deviates slightly from the M3 points at cooler temperatures, just as does the bulk of the NGC 6981 variables. Comparison of the points, directly, shows the equality.) Because the period shifts are the same at all temperatures for all variables, the van Albada–Baker hysteresis

[1]Note again that this will not be true in van Albada and Baker's (1973) hysteresis model for the transition period, hence our requirement is an observational test that can decide between the models.

[2]Strict coincidence of the amplitude-temperature relations requires that the instability strip be vertical in the H-R diagram, rather than be sloped toward cooler temperatures for brighter magnitudes. This, however, is observed to be the case between group I and group II clusters (SKS 1981, and Table 7 discussed later here) and was shown in Paper I to require a difference in the He abundance.

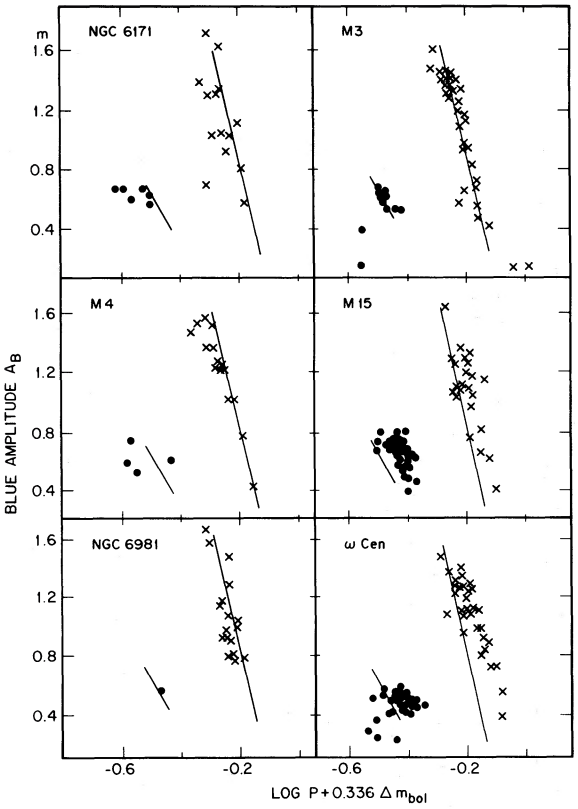

FIG. 3.—Blue amplitude–reduced period relations for the six clusters. The approximate linear fits through the M3 data are repeated in all panels.

model does not explain the shifts nor, therefore, the Oosterhof groups.

The second important feature of Figure 2 is the lack of overlap in temperature between the *c* and *ab* variables for the first four clusters and the large overlap of *ab* and *c* types for M15 and ω Cen but not for M3, provided that a hysteresis occurs in the mode change as calculated by Stellingwerf (1975). However, an adequate model is yet to be found.

The data in Figure 3 show that similar period shifts occur in the period-amplitude relation. Again, the lines are taken to be the best linear fit to the M3 data. The sense of the period shifts is the same as from the $P-T_e$ relation. The summary in Table 7 (col. [11]) gives $\Delta\log P$ values of +0.053, +0.030, 0.000, −0.055, and −0.045 for NGC 6171, M4, NGC 6981, M15, and ω Cen, respectively.

As discussed in Paper I, the period shifts can also be determined from the light curve shapes. The data are plotted in Figure 4 where inspection shows that $\Delta\log P$ determined here are generally the same as derived from Figures 2 and 3. The lines in Figure 4 are from M3. These period shifts are listed in column (12) of Table 7.

Other relevant data for the six clusters are also summarized in Table 7. The *ab* mean periods are in column (2). The [Fe/H] from Zinn (1980) are in column (3). The adopted reddenings in column (4) are from Paper III, to follow. Columns (5) and (6) give the reddening-corrected colors of the blue and red edges of the instability strip. The gap boundary temperatures are on the $T_e(2)$ scale based on $[\langle B\rangle-\langle V\rangle]_0^c$ colors of the reddest and bluest variables.

The first harmonic blue edge (i.e., for *c* variables) has nearly the same temperature for all clusters. Because the slope of the color-temperature relation is $\Delta(B-V)\approx 3\Delta\log T_e$, agreement of the blue edge temperatures to within $\Delta\log T_e\approx\pm 0.003$ implies agreement of the *blanketing corrected* colors to within $\Delta(B-V)\approx\pm 0.01$ mag, which is the observational error. Hence, the blue boundaries of the instability strip are nearly vertical, despite the difference in absolute luminosity of ~0.4 mag between ω Cen and NGC 6171 that is needed to explain $\Delta\log P=0.12$. Note again that a vertical strip also requires a difference in helium content such that He(ω Cen)>He(NGC 6171) (cf. SKS in Paper I, eq. [10]).

The shifts in the amplitude-temperature and rise time–temperature relations are listed in columns (14) and (15) of Table 7. These, according to the model, should be zero, and they very nearly are. Hence, from this and from the similarity of the $\Delta\log P$ values from the *P-A*, $P-\Delta\phi$ rise, and $P-\log T_e$ relations, we conclude that the requirements of the present luminosity-difference model of the Oosterhof problem are met for the six clusters.

We now inquire more closely into (1) the intrinsic scatter of Figure 2, (2) the question of the mass term in equation (1), and (3) the evidence for a period-luminosity-amplitude relation.

IV. INTRINSIC DISPERSION IN ABSOLUTE MAGNITUDES AND MASSES OF RR LYRAES IN A GIVEN CLUSTER

a) Theoretical Expectations

i) *Mass Variations*

The horizontal branch is believed to be populated by stars that have left the tip of the giant branch immediately after the core has begun to burn helium into carbon and oxygen. Such stars distribute themselves along the ZAHB according to their total mass, which, from the models, is required to be a free stochastic parameter so as to populate the HB along its entire length.

The model calculations of Iben and Rood (1970, Fig. 6), Sweigart and Gross (1976), and Caloi, Castellani, and Tornambè (1978, Figs. 9 and 10), show that the

TABLE 7

GAP CHARACTERISTICS FOR FIVE CLUSTERS OF DIFFERENT METALLICITY

NAME NGC (M)	⟨Pab⟩	$[Fe/H]_z$	E(B-V)	$(B-V)^\circ_B$	$(B-V)^\circ_R$	Log T_e: Gap Boundaries				Δ log P			Δ log T_e	
						B_c	R_c	B_{ab}	R_{ab}	P-A	P-Δφ	P-log T_e	A-T_e	Δφ - T_e
(1)	(2)	(3)	(4)	(5)	(6)	(7)	(8)	(9)	(10)	(11)	(12)	(13)	(14)	(15)
5272 (3)	$0^d.551$	-1.69	$0^m.00$	$0^m.20$	$0^m.45$	3.876	3.850	3.853	3.791	0.000	0.000	0.000	0.000	0.000
6121 (4)	0.538	-1.46	0.36+δ	(0.18)	(0.40)	(3.880)	(3.860)	3.857	3.806	+0.030	+0.035	0.000	-0.004	-0.004
6171 (··)	0.527	-0.89	0.28	0.20	0.51	3.879	3.834	3.850	3.780	+0.053	+0.065	+0.060	+0.008	+0.004
6981 (72)	0.552	-1.58	0.04	(0.22)	0.43	. . .	. . .	3.863	3.788	0.000	-0.010	-0.010	-0.006	(-0.010)
7078 (15)	0.640	-2.15	0.08	0.17	0.41	3.876	3.818	3.879	3.794	-0.055	-0.055	-0.070	0.000	0.000
ω Cen	(0.65)	-2	0.11	0.15	0.37	3.882	3.826	3.876	3.807	-0.045	-0.060	-0.070	~0.0	~ 0.0

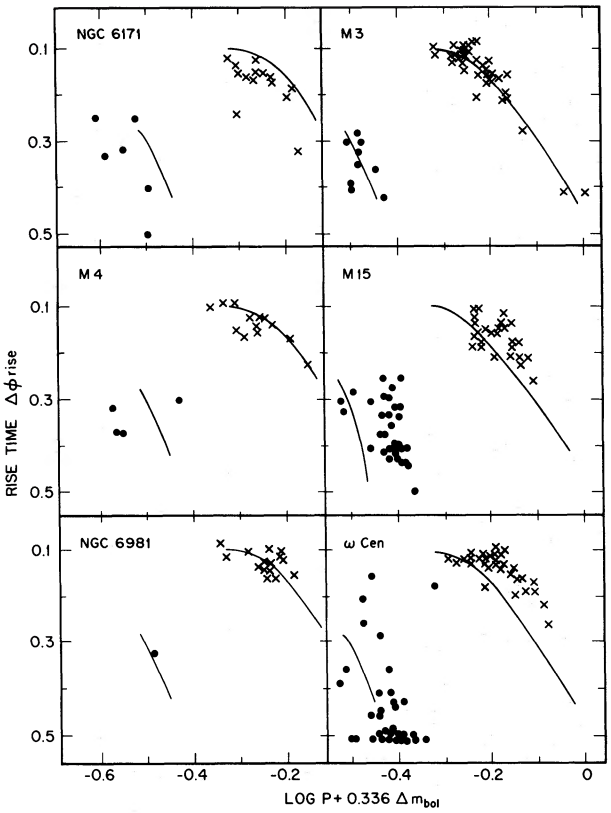

FIG. 4.—The reduced period–rise time relations for the six colors. Lines drawn by eye through the M3 data are repeated in all panels.

variation of mass within the instability strip of a given cluster has a gradient of

$$\left.\frac{\partial \log M}{\partial \log T_e}\right| \approx -0.33, \qquad (2)$$

read at $\log T_e = 3.84$, $Y = 0.25$, and $[Fe/H] = -1.7$. This particular value has been found from Figs. 9 and 10 of Caloi *et al.* The sense is that stars with cooler temperatures have higher masses. The gradient steepens both for lower metallicities and temperatures lower than $\log T_e \sim 3.83$, but equation (2) is sufficiently accurate to estimate the effect of mass variations on the period-temperature relation for RR Lyrae variables on or near the ZAHB in most clusters.

Adopting the width of the instability strip to be $\Delta \log T_e \approx 0.09$ and using equation (2), the predicted variation of mass for RR Lyrae stars with $[Fe/H] = -1.7$ is only

$$\Delta \log M \approx 0.03. \qquad (3)$$

This mass variation is expected to be systematic within the strip; i.e., it varies with T_e; hence, it should cause a slope change in the $\log P + 0.336\, \Delta m_{bol} = f(T_e)$ plots of Figure 2 via equation (1). Because the mass is higher for lower temperatures, the periods should be shorter than given by the slope of $\partial \log P'/\partial \log T_e = -3.48$ from equation (1). Substitution of equation (2) in (1) gives a predicted slope of $\partial(\log P + 0.336\ m_{bol})/\partial \log T_e = -3.25$. This is so similar to the slope of -3.48 drawn in Figure 2 that comparison of the prediction with the data provides only marginal evidence at best for a variation of mass with T_e. Therefore, the predicted variation of mass *across* the strip can be neglected.

More easily tested is a predicted variation of mass at a given T_e due to *evolution* away from the zero-age horizontal branch.

ii) *Variations of Mass and Luminosity due to Evolution at any Given T_e*

Evolutionary tracks from the ZAHB calculated by Iben and Rood (1970, Fig. 1) and Sweigart and Gross (1976, Figs. 1–6) show a maximum change in luminosity due to evolution of $\Delta \log L_{RR} \approx 0.2$. Because a number of evolutionary tracks from different parts of the ZAHB are in the strip at the same time, there should be a small mass-spread that accompanies the spread in luminosity. The most extreme cases given by both Iben and Rood and by Sweigart and Gross show that a vertical cut made at $\log T_e = 3.84$ (for $Y = 0.3$, $Z = 0.0001$, for example) in their diagrams encompasses tracks that have a spread of $\Delta \log L = 0.22$. These tracks start from various parts of the ZAHB whose mass interval is from $M = 0.62$ to $M = 0.75$, or $\Delta \log M \approx 0.08$.

To be sure, most of the observed variables will have a smaller mass range because those near the low mass end of the interval will pass through the strip rapidly and hence will be rare. A more realistic expected mass range for $\sim 90\%$ of the RR Lyrae stars in any cluster is read from the quoted diagrams to be $\Delta \log M \approx \pm 0.02$. From equation (1), this should result in an additional scatter over and above the observational errors of $\Delta \log P' \approx \pm 0.014$, read in Figure 2 at constant T_e.

b) Observational Tests

i) *Can Luminosity and Mass Variations Be Detected from the Dispersion in the Period-Temperature Relation?*

Figures 5–7 show the period-temperature relations from Tables 2–6, plotted with the observed periods in the left panels, and the reduced periods on the right. As before, the correction for bolometric magnitude has been normalized to be zero for each cluster in the mean.

Figure 5 shows the data for M15 and NGC 6171. There is, in each case, a slight improvement in the right hand panels. How much is expected? Variations of the RR Lyrae luminosities of 0.1 mag in any given cluster

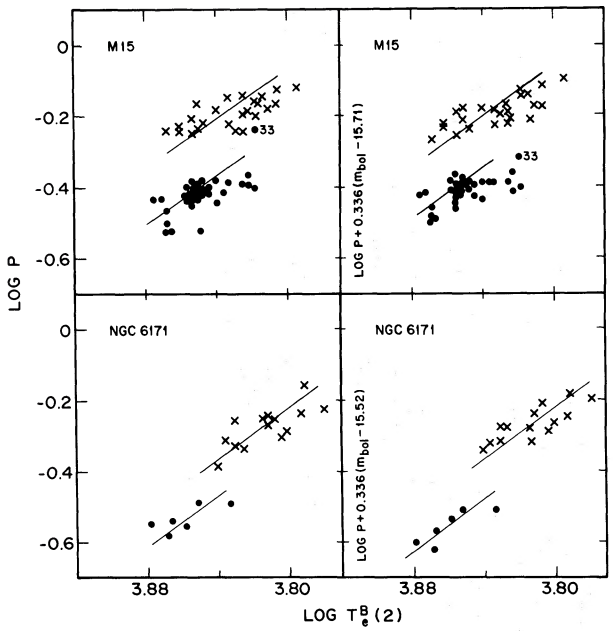

FIG. 5

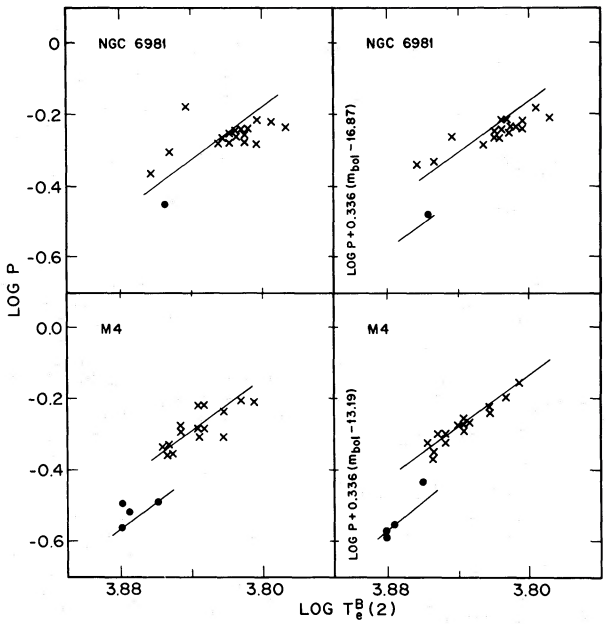

FIG. 6

FIG. 5.—Period-temperature relations for M15 and NGC 6171 showing the decrease in scatter using the reduced periods (*right panels*) compared with the observed periods (*left panel*). Lines have been drawn by eye through the points using the theoretical slope of 3.48 from eq. (1), assuming constant mass. Data are from Table 6 of SKS (1981) and Table 4 here.

FIG. 6.—Same as Fig. 5 for NGC 6981 and M4, using data from Tables 3 and 5

translate via equation (1) to deviations of $\Delta \log P = 0.03$ at any given T_e. This amount is small but, given the size of the $P(T_e)$ variation, should be just detectable in Figures 5–7; as it is. A very much more powerful test for a range of luminosities in a given cluster is made in the next section.

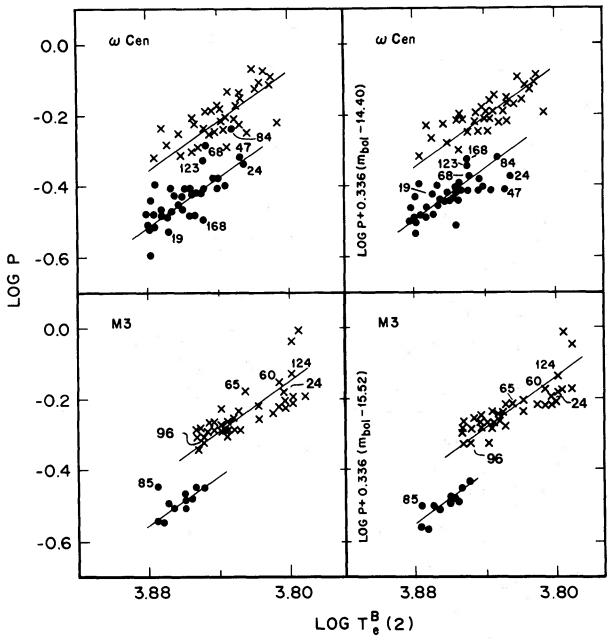

FIG. 7.—Same as Fig. 5 for M3 and ω Cen, using data from Tables 1 and 6. Stars discussed later in Figs. 8–11 are marked.

What now about the mass? The remaining scatter in the *right* panels of Figures 5–7 is of the order $\Delta \log P' \approx \pm 0.04$ for most of the clusters. The variation is $\Delta \log T_e \approx \pm 0.01$ when read as dispersion in the abscissa which, if taken to be due to errors in color, requires $\varepsilon(B-V) = \pm 0.03$. This is about $1\frac{1}{2}$ times the observational error, hence some small margin is left for variations in mass at a given T_e. The expectation is $\Delta \log P' = \pm 0.014$ due to the mass variation as estimated in the last section. When this is combined with an error of $\Delta \log T_e = \pm 0.006$ due to observational errors of $\varepsilon(B-V) = \pm 0.02$, we obtain the expected scatter to be $\Delta \log P \approx \pm 0.03$, which is close to what is observed.

Hence, the scatter in the right-hand panels of Figures 5–7 is not smaller than required by the observational errors, but not larger than can be accounted for by the small but finite dispersion in mass at fixed T_e that is predicted.

ii) *First Harmonic Pulsators Masquerading as* ab *Variables*

We close this section by noting a class of stars isolated in M15 and ω Cen from Figures 5 and 7 that, at first glance, appear to be *ab* variables but may, in fact, be pulsating in the first overtone. Four such stars, listed in Table 8, have longer periods than usual for *c* vari-

TABLE 8

FIRST HARMONIC PULSATORS MASQUERADING AS *ab* VARIABLES

Name	r''	P (days)	A_B (mag)	$\Delta\varphi_{rise}$
M15-33	51	0.583	1.17	0.15
ω Cen-68	632	0.534	0.52	0.50
ω Cen-84	1205	0.579	0.81	0.17
ω Cen-123 ...	516	0.473	0.49	0.50

ables, and at least two (M15-33, ω Cen-84) have large amplitudes and asymmetric light curves. The reason for believing them to be overtone pulsators is that all fall among the *c* variables in the ($\log P, \log T_e$)-plane when corrected for their brighter than average luminosity in the right-hand panels of Figures 5 and 7.

The case for M15-33 is weak because the star is close to the cluster center and the contamination corrections are uncertain (SKS). However, the case for the three ω Cen variables is strong because uncertainties in their photometry should be small. The very long periods of these *c*-type stars is of interest. These abnormal periods are due entirely to their bright luminosities.

V. THE *P-L-A* RELATION FOR M3 AND ω CENTAURI

a) The Observed Magnitude Spread in M3 and ω Centauri Is Real

If the observed spread in apparent magnitude of RR Lyrae variables in a given cluster is real, brighter variables should have longer periods than fainter ones at the same T_e. The test is very powerful, and is made here for M3 and ω Cen separately.

The upper panel of Figure 8 shows the instability strip for M3 using data in Table 1. A few stars near the extremes of luminosity are marked here, as well as in Figure 7 and Figure 11 to be discussed.

For the dispersion to be real, the brightest stars in Figure 8 should be near the upper boundary of the points in Figure 7*a*, but should not deviate systematically in Figure 7*b*. This is indeed the case. The five brightest variables, 96, 65, 60, 24, and 124, move toward shorter reduced periods in the right-hand panel of Figure 7, as required. Figure 10, discussed later for the complete M3 sample, shows the correlation between m_{bol} and $\Delta \log P$ to be general.

Similar data for ω Cen are shown in Figure 9 where, because of the large temperature overlap between the modes, the *c* and *ab* variables are plotted separately. The variables are also coded separately by metallicity, according to Table 6.

As in Figures 7 and 12 (shown later), a few individual bright and faint stars are identified in Figure 9. In a way similar to that for M3, inspection of Figure 7 shows that the brightest *ab* variables in Figure 9 have longer periods than fainter stars at equal T_e, and hence form the upper envelope of the distribution in the left panel of Figure 7, but merge with the mean distribution in the right panel.

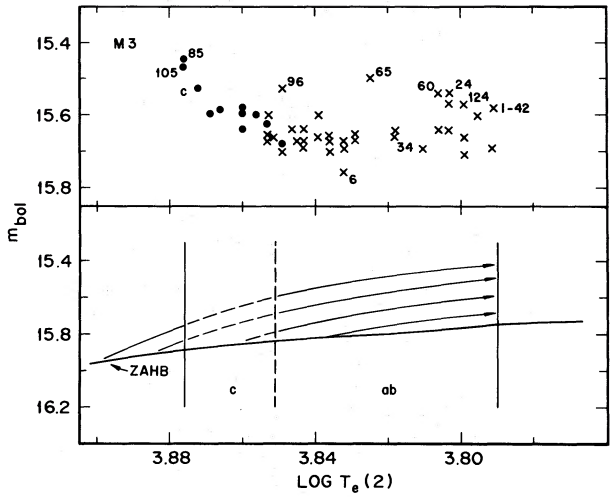

FIG. 8.—*Top*, The observed ($m_{bol}, \log T_e$)-diagram for variables in M3 from data in Table 1. Type *c* variables are circles; *ab* variables are crosses. Particular variables are marked. *Bottom*, *schematic* representation of four evolutionary tracks from the zero-age main sequence that cross the instability strip. The tracks are dashed in the domain of the *c* type variables; are solid in the *ab* domain. No hysteresis in the mode change can be permitted because there is no observed overlap in temperature between *c* and *ab* variables in the upper panel.

The correlation of period residuals and apparent magnitudes for all variables in M3 and ω Cen is shown in detail in Figure 10. The $\Delta \log P$ values have been determined from the scatter in period of each star from the mean fiducial *period-amplitude* relation for each cluster. This relation is subject to less observational error than the *P-T*$_e$ relations of Figures 5 and 7 because amplitudes need only be determined to $\sim \pm 0.1$ mag, whereas colors must be known to $\sim \pm 0.01$ mag for similar accuracy in $\Delta \log P$. These $\Delta \log P$ values are listed in columns (14) and (11) of Tables 1 and 6, respectively; m_{bol} values are from the same tables.

The lines in Figure 10 are placed by eye with a slope given by

$$\Delta m_{bol} = 3 \Delta \log P, \qquad (4)$$

which follows from equation (1) for fixed mass and temperature. Because amplitude is a unique function of temperature (see the next subsection), the condition of fixed T_e is equivalent to determining $\Delta \log P$ at fixed amplitude, as has been done from the *P-A* relation.

As the lines fit the data well for both clusters, the two principal conclusions are: (1) equation (1) is verified, and (2) the observed spread in L_{RR} for the M3 and for the ω Cen variables is real.

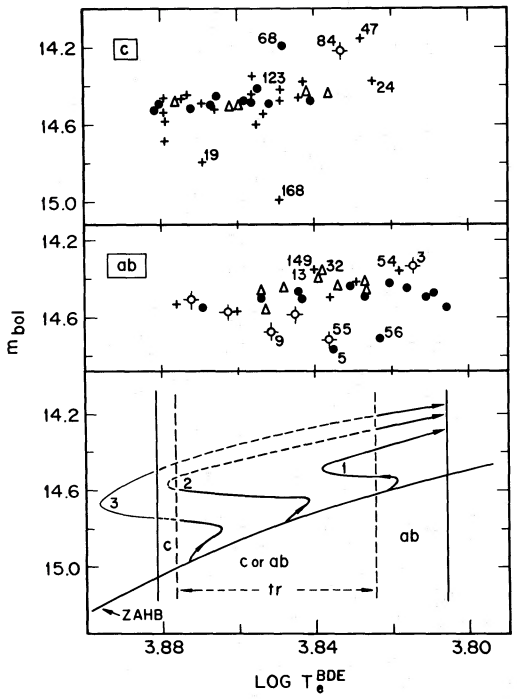

FIG. 9.—Same as Fig. 8 but for ω Cen, using data from Table 6. The *c* and *ab* variables are plotted separately in the top two panels. Crossed open circles are for metallicities in the interval $-0.5>[Fe/H]>-1.1$; triangles are for $-1.1>[Fe/H]>-1.6$; closed dots are for $-1.6>[Fe/H]>-2.3$; vertical crosses are of unknown metallicity. *Schematic* evolutionary tracks from a ZAHB are shown in the lower panel. Segments in the *c* domain are dashed, otherwise they are solid. If a hysteresis occurs in the mode change, an overlap in temperature between the *c* and *ab* types is a natural consequence.

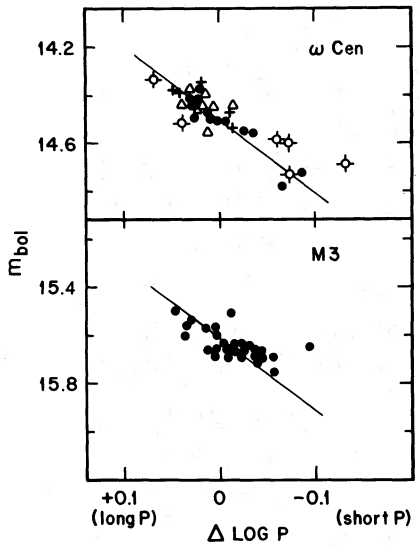

FIG. 10.—Correlation between the bolometric magnitudes and the period shifts of individual stars from the ridge-line *P-A* relations in M3 and in ω Cen. The data are from Tables 1 and 6. The lines have been drawn by eye, using equation (4) whose slope is 3.

Finally, a comment can be made concerning the overlap in temperature of the *ab* and *c* types in ω Cen, and its lack in M3. Schematic representations of evolutionary tracks that could lead to such a difference are shown in the lower panels of Figures 8 and 9 where portions of the tracks that produce *ab* variables are solid, and those that produce *c* types are dashed. A hystereris in the mode change is required to produce an ambiguous *zone* where the stars are either *c* or *ab* types,[3] and, further, no large transition zone is permitted in clusters such as M3.

b) Another Representation: Scatter in the P-A Relation

A different representation of the same results is shown in Figures 11 and 12 where the period-amplitude relations are given, first using the observed periods, and then, in an adjacent panel, using periods corrected for luminosity differences via equation (1). The reduction of scatter, depending on the m_{bol} of the individual stars, is evident for both clusters. Individual stars marked in Figures 8 and 9 are also marked here to show that brighter stars than normal have longer periods at given amplitudes than fainter ones. This is just the condition predicted by equation (1), providing that amplitude is a unique function of T_e.

Again, the conclusions to be drawn from these data are:

1. Stars of brighter absolute magnitude have longer periods than others of the same temperature (Figs. 5 and 7) via equation (4).
2. Stars of the same amplitude but different period have different absolute magnitudes (cf. Fig. 10), also given by equation (4).
3. Conclusions (1) and (2), taken together, require amplitude to be a unique function of temperature (as is directly observed from color-amplitude relations: cf. Sandage 1981*a*, Fig. 4).

c) Explicit Form for the P-L-A Relation

If the mass variation is ignored and if amplitude is substituted as a function of temperature in equation (1), then

$$\log P + 0.336\, M_{bol} = g(A), \qquad (5)$$

where $g(A)$ is the monotonic amplitude-temperature relation. The form of $g(A)$ for *ab* stars is given by the curve that satisfies, in the mean, the points in the right

[3] If this *is* the explanation of the temperature overlap, we should note that the *predicted* width of the either/or transition zone is only 300° (Stellingwerf 1975), which is much smaller than the observed width of $\Delta T_e \simeq 800°$ from Figure 9. Only part of the discrepancy can be due to errors in the colors. After correction for $\epsilon(B-V) \simeq \pm 0.02$, the remaining width is about two times larger than predicted. Hence, either this explanation for the temperature overlap is suspect, or the model calculation may not be precise.

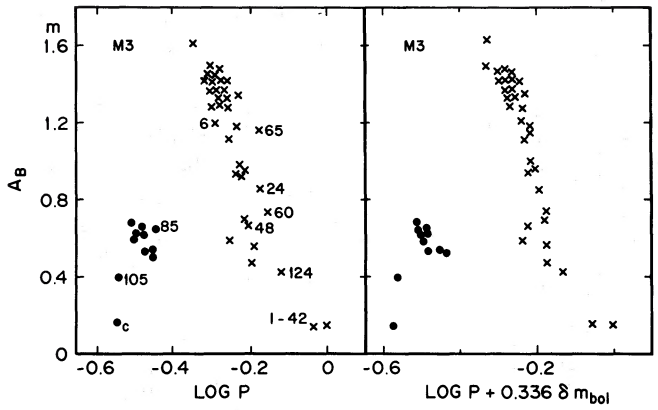

FIG. 11.—Amplitude-period relation for M3. Observed periods are used in the left panel, reduced periods on the right.

panel of Figure 11 for M3, or the top panel of Figure 12 for ω Cen. Adopting the ridge-line *P-A* relation for M3 as the standard template and, to fix ideas, linearizing, gives the fiducial *P-A* relation as

$$\log P = -0.129\, A_B - 0.088. \quad (6)$$

It follows from equation (5) that

$$g(A) \equiv -0.129\, A_B - 0.088 + 0.336\, M_{\rm bol}(M3_{15.52}), \quad (7)$$

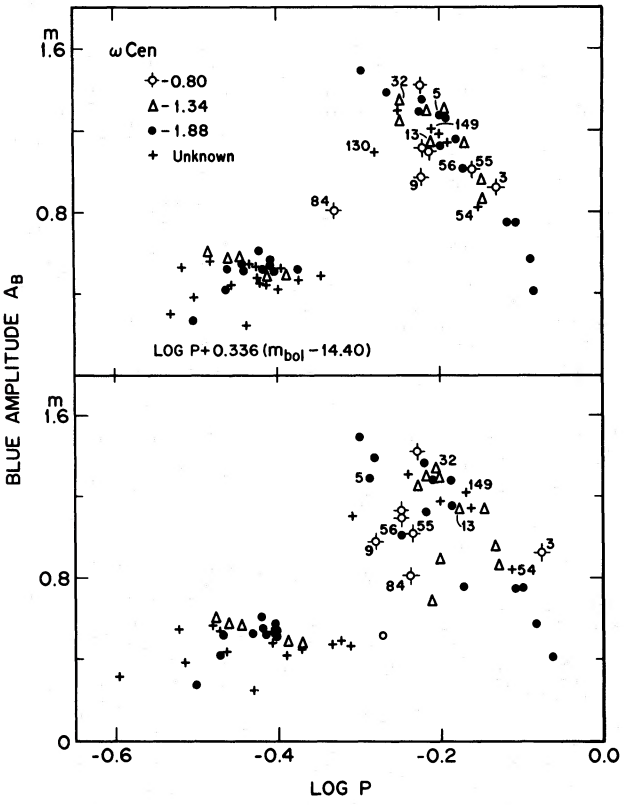

FIG. 12.—Same as Fig. 11 but for ω Cen. Coding for the different metallicities is the same as in Fig. 9.

where $M_{\rm bol}(M3_{15.52})$ is the absolute bolometric magnitude of variables in M3 whose apparent bolometric magnitude is 15.52. This is the normalization that makes $\Sigma\, \Delta m_i({\rm bol}) = 0$ for the M3 RR Lyrae stars (see the ordinate of the right panel of Fig. 7), and hence is that which has been used in Fig. 11 (right panel), and therefore is implicit in equation (6).

Substitution of equation (7) into (5), now to be applied to any variable of period P and amplitude A_B, gives

$$M_{\rm bol} = M_{\rm bol}(M3_{15.52}) - 3.0[\log P + 0.129\, A_B + 0.088]. \quad (8)$$

Because we do not yet know the distance modulus to M3 accurately, equation (8) only gives absolute magnitudes of any variable relative to those in M3 whose $m_{\rm bol} = 15.52$. The *absolute* calibration must await programs yet in progress that include new statistical parallax determinations that use equation (8) to produce better reduced proper-motion values for field variables, or by several Baade-Wesselink programs currently in progress.

d) *Effect of Variation of Mass with* [Fe/H]

The principal uncertainty in equation (8) is the neglect of the mass term in the generating equation (1). The arguments in § IV show that the neglect is justified in any *given* cluster of homogeneous metallicity, but may not be justified from one cluster to another whose metallicity differs from M3, for the following reason.

The cited models show that the mass at any given T_e on the ZAHB is sensitive to Z; the lower the metallicity the higher is the mass at the T_e. Figures 9 and 10 of Caloi, Castellani, and Tornambè (1978) are useful to show that at fixed T_e near $\log T_e = 3.85$, with Y between 0.2 and 0.3, mass varies with Z as

$$\partial \log M / \partial \log Z = -0.066. \quad (9)$$

The effect that this variable mass with different Z has on $\Delta \log L_{RR}$ between M3 and M15 is discussed in Paper I (SKS, § IV). We generalize that discussion here.

It will be shown in Paper III (Sandage 1981*b*), using data for 30 clusters, that $\Delta \log P$ for variables in any given cluster relative to M3 is a tight function of $\log Z$, given by

$$\Delta \log P = -0.112 \Delta \log Z, \tag{10}$$

in the the sense that low metallicity clusters have variables of longer period at a given amplitude. This is a generalization of the initial discovery by Arp (1955) that clusters of the long-period Oosterhoff group II have lower metallicities than clusters of group I. If, then, clusters of lower metallicity have higher mass for their RR Lyrae stars on the ZAHB, equation (1) shows that they must have an even brighter ZAHB than would be given by $\Delta M = 3\Delta \log P$. The needed increased HB luminosity difference that would produce a given $\Delta \log P$ follows by combining equations (9) and (10) with (1) to obtain, at fixed T_e,

$$\Delta M_{bol} = 4.2 \Delta \log P, \tag{11}$$

again in the sense that longer-period RR Lyrae variables must have brighter absolute magnitudes.[4]

If this mass variation with metallicity is correct, the equivalent of equation (8) becomes

$$M_{bol} = M_{bol}(M3_{15.52}) - 4.2[\log P + 0.129 A_B + 0.088]. \tag{12}$$

One test of equation (9) should, in principle, be available using the upper panel of Figure 10 where ω Cen variables with a range in surface metallicity are plotted. If $M = f(z)|_{T_e}$ via equation (9), there should be a systematic difference along the abscissa between the open spiked circles and the closed dots by $\Delta \log P = 0.068(0.066) = 0.04$, according to equations (1) and (9) using $\Delta \log Z = 1$. The closed circles should be shifted systematically rightward by this amount. However, Figure 10 shows that this shift is not present. There are three possibilities: (1) equation (9) is wrong, (2) the observed surface variation of [Fe/H] for ω Cen variables is not an interior abundance difference, in which case ω Cen RR Lyrae stars can provide no observational test of equations (9), (11), and (12), or (3) the C+N+O abundance, which is the important "Z" for RR Lyrae variables, may not vary with the "[Fe/H]" that is measured by the ΔS technique. We cannot decide from the presently available data which of these alternatives is correct. Although we could carry forward two parallel analyses in Paper III, one using equation (4) and the other equation (11), the practical difference between the solutions is nearly negligible; hence we adopt equation (4) in the sequel.

A subtle but important point must now be emphasized concerning the difference between equations (8) and (12). Equation (8), whose parents are equations (1) and (4), is expected to apply in any circumstance where the mass of the RR Lyrae stars under consideration is the same. To be specific, equation (8) should be valid when differences occur in L_{RR} due, for example, to evolution in a sample of stars with the same metallicity. According to the cited models, this should be a nearly constant mass case. Note particularly that even in ω Cen where [Fe/H] varies from star to star, the slope of $\partial M_{bol}/\partial \log P$ should still be 3.0 as in equations (4) and (8) for *each* metallicity group.[5]

Equation (12) has a quite different, rather hybrid, meaning. It applies to the case where L_{RR} differs *between* clusters for variables that are on or near their respective ZAHBs. The reason for the L_{RR} difference lies not in the evolution, as is the case *within* a given cluster, but rather with the much deeper cause of the Oosterhoff period phenomenon itself that produces different luminosity levels for ZAHBs in different clusters. While an explanation of that cause is most fundamental for an understanding of the history of the globular cluster system (Paper III), all we need to understand here is that, *given* the *empirical* connection between $\Delta \log P$ and Z for the system of globular clusters, via equation (10) no matter what its explanation, and *given* the (M, Z) dependence of equation (10), we must have the *larger* $\Delta \log L_{RR}$ between clusters of different metallicity as given by equation (11) rather than by equation (4).

In different words: the deeper meaning of equation (10) lies at the heart of the problem of the Oosterhoff groups. But given the empirical fact that the $(\Delta \log P, Z)$ correlation does exist between the clusters, we need not understand here why it is so, but nevertheless must use equation (11) to compare one cluster (or one field RR Lyrae star) with another, provided that equation (9) is correct.

VI. A COMMENTARY

Although very different in appearance, the analysis given here and in Paper I for RR Lyrae stars is identical in principle to that given earlier for the longer-period Cepheids, where it was shown that a third parameter is also necessary to describe their periods and luminosities (Sandage 1958*b*, 1972) due to the finite width of the

[4] It can be shown from the models of Sweigart and Gross that the variation of RR Lyrae mass with Y at fixed [Fe/H] and T_e is small enough to be neglected, both in the discussion in § IV and in the result contained in equation (11).

[5] The prediction via equation (9) is not that the slope in Figure 10 should change to 4.2, but rather that there should be a series of parallel lines in that diagram all of slope 3 but separated according to log Z. It is the absence of such a separation that lends suspicion that equation (9) shows too strong a dependence.

instability strip. What makes the RR Lyrae and the longer-period Cepheid cases *appear* to be different is that the relative importance of the three parameters is itself so different in each regime.

In the RR Lyrae case, the luminosities are very nearly the same for all variables. This is because (1) the evolutionary tracks threading the instability strip *are* nearly horizontal, and (2) all clusters are nearly the same age, hence their horizontal branches, although not identical in L_{RR}, vary in L by less than $\Delta \log L_{RR} \approx 0.3$ (cf. Paper III).

Nevertheless, there *is* a range of periods for the RR Lyrae variables, albeit small, due to *position in the gap*, which is the third parameter. Hence, in the RR Lyrae regime, period is hardly a function of luminosity but is a strong function of gap position, measured either by color or by its equivalent amplitude.

The case of the long-period Cepheids is different only because their progenitor main-sequence parents have a *large range in age*, hence their Cepheid daughters populate the H-R diagram over the very wide range in luminosity of $\Delta \log L \gtrsim 2$. Because the width of the instability strip is so narrow compared with its large extent in L, the *P-L* relation alone is the dominant correlation here; i.e., the color (or amplitude) term is very small. Nevertheless, this third parameter can be detected in the classical Cepheids (Sandage and Tammann 1968, 1969), and it exhibits the same quantitative behavior as in the RR Lyrae regime—viz., amplitude decreases monotonically toward redder colors (Cogan 1980), a circumstance which leads there, as here, to a *P-L-A* relation (Sandage and Tammann 1971). These developments of the *P-L-T* relation or its equivalent *P-L-A* function, both for the RR Lyrae variables and for the classical Cepheids, are based solely on the requirement that (1) $P\langle \rho \rangle^{1/2} \approx$ constant, and (2) the instability strip has a very small, yet finite, temperature width for all values of L.

It is a pleasure to thank Nancy Newton and Pamela Gilman for their characteristically fine work in preparing the diagrams and manuscript for publication. I am especially grateful to Dr. Horace Smith who pointed out an error in an early draft.

REFERENCES

Arp, H. C. 1955, *A.J.*, **60**, 317.
Baker, R. H., and Baker, H. V. 1965, *A.J.*, **61**, 283.
Butler, D., Dickens, R. J., and Epps, E. 1978, *Ap. J.*, **225**, 148.
Cacciari, C. 1979, *A.J.*, **84**, 1542.
Caloi, V., Castellani, V., and Tornambè, A. 1978, *Astr. Ap. Suppl.*, **33**, 169.
Cogan, B. C. 1980, *Ap. J.*, **239**, 941.
Dickens, R. J. 1971, *Ap. J. Suppl.*, **22**, 249.
Dickens, R. J., and Flinn, R. 1972, *M.N.R.A.S.*, **158**, 99.
Dickens, R. J., and Rolland, A. 1972, *M.N.R.A.S.*, **160**, 37.
Hogg, H. S. 1955, *David Dunlap Pub.*, Vol. **2**, No. 2.
_____. 1973, *David Dunlap Pub.*, Vol. **3**, No. 6.
Iben, I., and Huchra, J. 1972, *Astr. Ap.*, **14**, 293.
Iben, I., and Rood, R. T. 1970, *Ap. J.*, **161**, 587.
Martin, W. Chr. 1938, *Leiden Ann.*, Vol. **17**.
Preston, G. W. 1961, *Ap. J.*, **133**, 29.
Roberts, M. S., and Sandage, A. 1955, *A.J.*, **60**, 185.
Sandage, A. 1958*a*, in *Stellar Populations*, ed. D. O'Connell (*Ricerche Astr. Specola Vaticana*, Vol. **5**), p. 41.
Sandage, A. 1958*b*, *Ap. J.*, **127**, 513.
_____. 1959, *Ap. J.*, **129**, 596.
_____. 1969, *Ap. J.*, **157**, 515.
_____. 1972, *Quart. J.R.A.S.*, **13**, 202.
_____. 1981*a*, *Ap. J.* (*Letters*), **244**, L23.
_____. 1981*b*, *Ap. J.*, in press (Paper III).
Sandage, A., and Katem, B. N. 1964, *Ap. J.*, **139**, 1088.
Sandage, A., Katem, B. N., and Sandage, M. 1981, *Ap. J. Suppl.*, **46**, in press. (SKS).
Sandage, A., and Tammann, G. A. 1968, *Ap. J.*, **151**, 531.
_____. 1969, *Ap. J.*, **157**, 683.
_____. 1971, *Ap. J.*, **167**, 293.
Stellingwerf, R. F. 1975, *Ap. J.*, **195**, 441.
Sturch, C. R. 1977, *Pub. A.S.P.*, **89**, 349.
Sweigart, A. V. and Gross, P. G. 1976, *Ap. J. Suppl.*, **32**, 367.
van Albada, T. S., and Baker, N. 1971, *Ap. J.*, **169**, 311.
_____. 1973, *Ap. J.*, **185**, 477.
Zinn, R. 1980, *Ap. J. Suppl.*, **42**, 19.

ALLAN SANDAGE: Mount Wilson and Las Campanas Observatories, 813 Santa Barbara Street, Pasadena, CA 91101